



Article

Transient Receptor Potential Vanilloid 4-Dependent Microglial Function in Myelin Injury and Repair

Jameson P. Holloman ¹, Sophia H. Dimas ², Angela S. Archambault ¹, Fabia Filipello ¹, Lixia Du ³, Jing Feng ³ , Yonghui Zhao ³, Bryan Bollman ¹, Laura Piccio ^{1,†}, Andrew J. Steelman ^{2,4} , Hongzhen Hu ^{3,*,‡} and Gregory F. Wu ^{1,5,*}

- ¹ Department of Neurology, Washington University School of Medicine, Saint Louis, MO 63110, USA; filipelof@wustl.edu (F.F.)
- ² Department of Animal Sciences, University of Illinois at Urbana-Champaign, Urbana, IL 61801, USA; shdi222@uky.edu (S.H.D.)
- ³ Department of Anesthesiology, The Center for the Study of Itch and Sensory Disorders, Washington University School of Medicine, St. Louis, MO 63110, USA; yonghuizhao@wustl.edu (Y.Z.)
- ⁴ Department Neuroscience Program, Division of Nutritional Sciences, and Carl R. Woese Institute for Genomic Biology, University of Illinois at Urbana-Champaign, Urbana, IL 61801, USA
- ⁵ Department of Pathology and Immunology, Washington University School of Medicine, Saint Louis, MO 63110, USA
- * Correspondence: hongzhen.hu@mssm.edu (H.H.); wug@neuro.wustl.edu (G.F.W.)
- † Current address: Charles Perkins Centre and Brain and Mind Centre, School of Medical Sciences, The University of Sydney, Camperdown, NSW 2050, Australia.
- ‡ Current address: Mark Lebwohl Center for Neuroinflammation and Sensation, Icahn School of Medicine at Mount Sinai, New York, NY 10029, USA.

Abstract: Microglia are found pathologically at all stages of multiple sclerosis (MS) lesion development and are hypothesized to contribute to both inflammatory injury and neuroprotection in the MS brain. Transient receptor potential vanilloid 4 (TRPV4) channels are widely expressed, play an important role as environmental sensors, and are involved in calcium homeostasis for a variety of cells. TRPV4 modulates myeloid cell phagocytosis in the periphery and microglial motility in the central nervous system. We hypothesized that TRPV4 deletion would alter microglia phagocytosis in vitro and lessen disease activity and demyelination in experimental autoimmune encephalitis (EAE) and cuprizone-induced demyelination. We found that genetic deletion of TRPV4 led to increased microglial phagocytosis in vitro but did not alter the degree of demyelination or remyelination in the cuprizone mouse model of MS. We also found no difference in disease in EAE following global or microglia-specific deletion of *Trpv4*. Additionally, lesioned and normal appearing white matter from MS brains exhibited similar *TRPV4* expression compared to healthy brain tissue. Taken together, these findings indicate that TRPV4 modulates microglial activity but does not impact disease activity in mouse models of MS, suggesting a muted and/or redundant role in MS pathogenesis.

Keywords: multiple sclerosis; disease activity; transient receptor potential vanilloid 4; TRPV4; microglia; inflammation; experimental autoimmune encephalitis; EAE; cuprizone



Citation: Holloman, J.P.; Dimas, S.H.; Archambault, A.S.; Filipello, F.; Du, L.; Feng, J.; Zhao, Y.; Bollman, B.; Piccio, L.; Steelman, A.J.; et al. Transient Receptor Potential Vanilloid 4-Dependent Microglial Function in Myelin Injury and Repair. *Int. J. Mol. Sci.* **2023**, *24*, 17097. <https://doi.org/10.3390/ijms242317097>

Academic Editor: David Della-Morte

Received: 18 September 2023

Revised: 1 November 2023

Accepted: 21 November 2023

Published: 4 December 2023



Copyright: © 2023 by the authors. Licensee MDPI, Basel, Switzerland. This article is an open access article distributed under the terms and conditions of the Creative Commons Attribution (CC BY) license (<https://creativecommons.org/licenses/by/4.0/>).

1. Introduction

Multiple sclerosis is the most common chronic inflammatory disease of the central nervous system (CNS) affecting an estimated 2.8 million people worldwide [1]. Although the exact etiology of MS is unknown, it is considered an autoimmune disease in which lymphocytes and peripheral macrophages infiltrate the brain and spinal cord and cause multifocal inflammatory lesions [2]. Neuropathological data has demonstrated that acute lesions contain T lymphocytes, B lymphocytes, plasma cells, activated microglia, and macrophages [3]. While the pathogenesis of MS was historically hypothesized to be driven

primarily by autoreactive T cells [4,5], a growing body of literature indicates a prominent role for microglia in MS [6].

Microglia have the potential to modulate MS disease activity in a variety of different ways via their diverse effector functions, including phagocytosis, antigen presentation, synaptic pruning, and the secretion of pro- and anti-inflammatory cytokines [7]. Microglia are found in high number in MS lesions and MS normal-appearing white matter (NAWM) [8]. In MS lesions, microglia are found surrounding the edge of active lesions and display an activated phenotype, suggesting they are important in plaque formation and tissue damage in MS [8]. Microglia have also been found within the MS brain in clusters termed “microglia nodules” that are associated with degenerating axons, stressed oligodendrocytes, and deposits of activated complement [9,10]. Microglia may also modulate the process of remyelination in MS. Phagocytosis of myelin debris by microglia promotes oligodendrocyte precursor cell differentiation and impacts the efficiency of remyelination [11]. Microglia-specific CX3CR1 knockout mice demonstrate reduced myelin clearance and decreased remyelination in the cuprizone mouse model [12]. Given this link between microglia and MS pathogenesis, a greater understanding of the cellular mechanisms underpinning microglial activation and function in MS will broaden our understanding of MS and may yield further therapeutic targets.

A growing body of literature indicates that the transient receptor potential (TRP) vanilloid 4 (TRPV4) channel modulates microglial activity in the context of neuroinflammation [13–16]. TRPV4 is a calcium-permeable, non-selective cation channel and a member of the TRP superfamily of cation channels [17]. TRPV channel dysfunction has been implicated in a variety of neurological disorders including MS [14]. TRPV1 stimulation has been found to induce an anti-inflammatory effect in microglia and MS patients with a TRPV1 single nucleotide polymorphism were found to have lower levels of pro-inflammatory TNF within their cerebrospinal fluid [18]. Within the TRPV receptor family, TRPV4 is the isoform most highly expressed in cortical microglia [19]. TRPV4 agonism has been found to increase neuroinflammation in an epilepsy mouse model [20] and increase blood–brain barrier permeability in endothelial cell culture [16]. On the other hand, TRPV4 antagonism has been found to decrease demyelination in the cuprizone mouse model [21,22]. Given the physiologic and therapeutic implications of TRPV4, further research into its role in MS is warranted.

We utilized *Trpv4* knockout mice to explore the impact of *Trpv4* deletion on neuroinflammation and demyelination observed in models of MS. We utilized both in vitro and in vivo model systems and analyzed TRPV4 expression in the brain tissue of MS patients. Our in vitro assay demonstrated increased microglia phagocytosis following *Trpv4* deletion but our experimental autoimmune encephalitis (EAE) and cuprizone animal models showed no impact of global or microglia-specific *Trpv4* deletion on disease severity or demyelination, respectively. We also observed no change in TRPV4 expression in MS lesions or NAWM compared to healthy control tissue. Taken together, these findings indicate that loss of TRPV4 increases microglia phagocytosis in vitro but that TRPV4 is unlikely to play a direct role in MS pathogenesis.

2. Results

2.1. *Trpv4* Deletion in Microglia Leads to Increased In Vitro Phagocytosis but Does Not Alter the Degree of Demyelination, Remyelination, or Microgliosis following Cuprizone Treatment

Microglia are hypothesized to facilitate repair following demyelination in MS via phagocytosis of myelin debris [12]. To determine if *Trpv4* deletion alters microglial phagocytosis, we performed an in vitro phagocytosis assay on microglia isolated from global *Trpv4* knockout (KO), or *Trpv4*^{KO}, mice. Loss of TRPV4 led to a 7.3% increase in the percentage of microglia performing phagocytosis (23.50% of *Trpv4*^{KO} microglia performed phagocytosis and 16.18% of wild-type (WT) microglia performed phagocytosis (95% CI, 0.15–13.04%), $p < 0.05$). *Trpv4*^{KO} microglia that engaged in detectable phagocytosis also contained a greater number of beads per cell compared to WT microglia (3.60 per microglia in

KO microglia (95% CI, 2.88–4.50) vs. 3.00 per microglia in WT microglia (95% CI, 2.04–3.95), $p < 0.05$) (Figure 1).

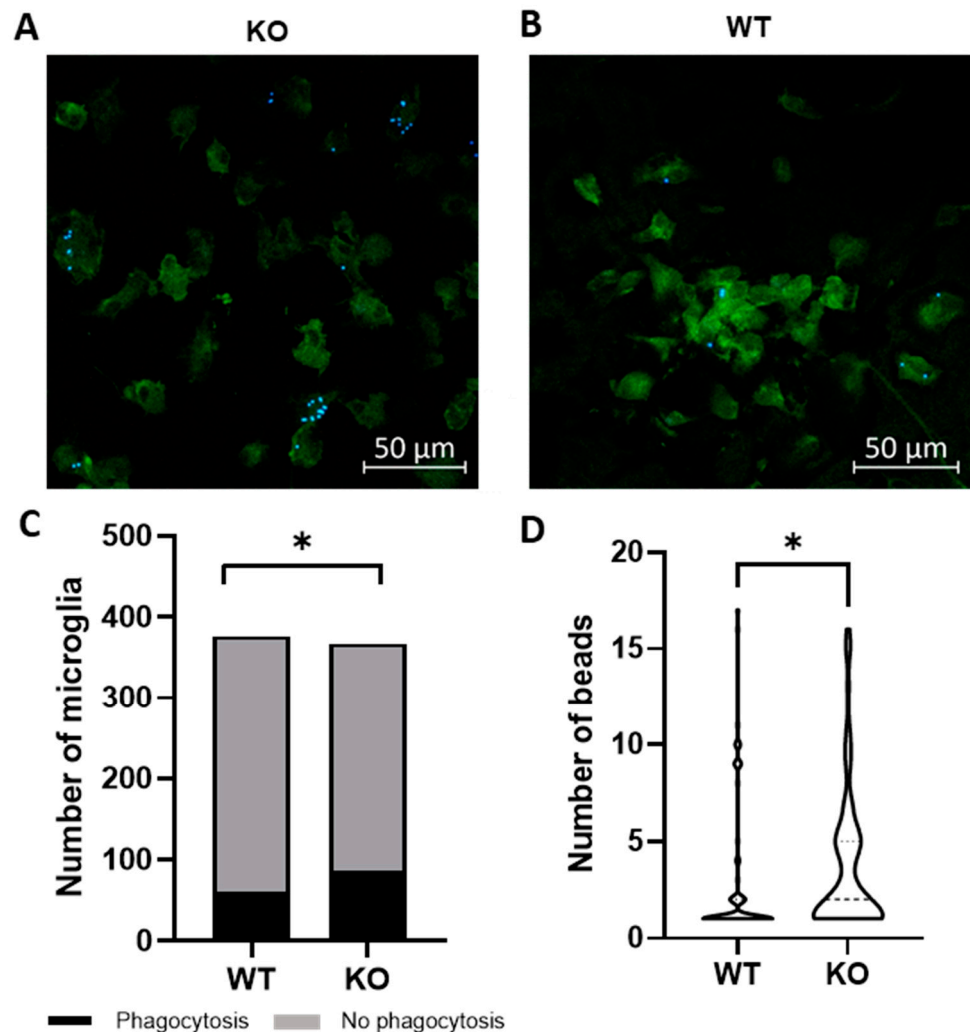


Figure 1. Global Trpv4^{KO} leads to increased microglia phagocytosis of fluorescent beads in vitro. (A,B) Microglia were cultured from P1-P3 global TRPV4^{KO} (A) and WT (B) mice and incubated with fluorescent latex beads for three hours to measure microglia phagocytosis. Green = Iba1, Blue = fluorescent latex beads. (C) Quantification of the number of microglia that phagocytose fluorescently labelled latex beads in vitro. (D) Quantification of the number of beads phagocytosed per microglia. Only microglia with at least one internalized bead were analyzed ($n = 64$ microglia in WT cohort and $n = 79$ in KO cohort). Scale bars indicate 50 μm . Statistical differences determined using a nested Student's t -test. Microglia were derived from ten different mice per experimental group. Two sets of cultures were obtained. * $p < 0.05$. WT = wild type microglia, KO = global TRPV^{KO} microglia.

Given the observed increase in phagocytosis in Trpv4^{KO} microglia, we next evaluated the impact of global Trpv4 deletion using the cuprizone mouse model to determine if this change translated to in vivo differences in demyelination and/or remyelination (Figure 2). Despite the difference in microglial phagocytosis in vitro, there was no difference in the degree of myelin loss following acute demyelination (6 weeks of cuprizone administration) in global Trpv4^{KO} mice (Figure 3). No difference in myelin basic protein (MBP) mean fluorescence intensity (MFI) was found when comparing Trpv4^{KO} and WT mice (94.20 in Trpv4^{KO} mice (95% CI, 21.74–49.17) vs. 104.10 in WT mice (95% CI, 23.83–58.96), $p = 0.64$). Similarly, myelin scoring in the splenium of the corpus callosum WT was found to be similar in

Trpv4^{KO} and WT mice (1.57 in Trpv4^{KO} mice (95% CI, 1.07–2.06) vs. 1.25 in WT mice (95% CI, 0.86–1.63), $p = 0.23$) (Figure 4).

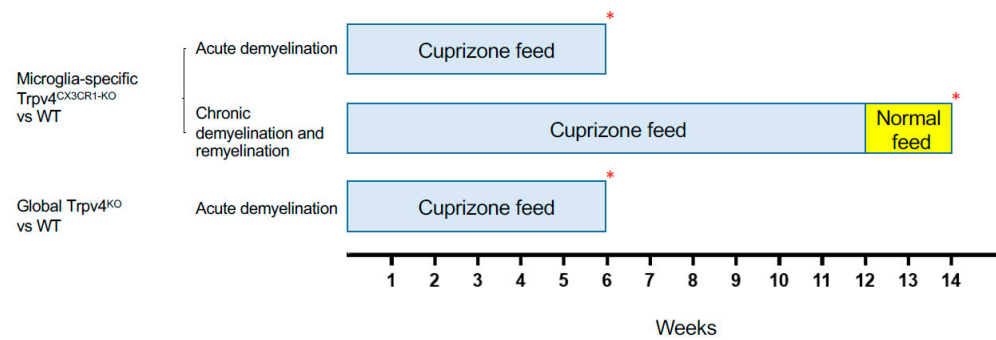


Figure 2. Schematic of the cuprizone protocols used to induce demyelination and remyelination in different experimental cohorts. Mice in the acute demyelination cohorts were fed cuprizone for 6 weeks and were then sacrificed and analyzed. Mice in the chronic demyelination and remyelination cohort were fed cuprizone for 12 weeks, normal feed for 2 weeks, and were then sacrificed and analyzed. Each experimental cohort was compared to a WT cohort that underwent the same protocol. The red asterisk (*) indicates the time point at which the mice were sacrificed. WT = wild type.

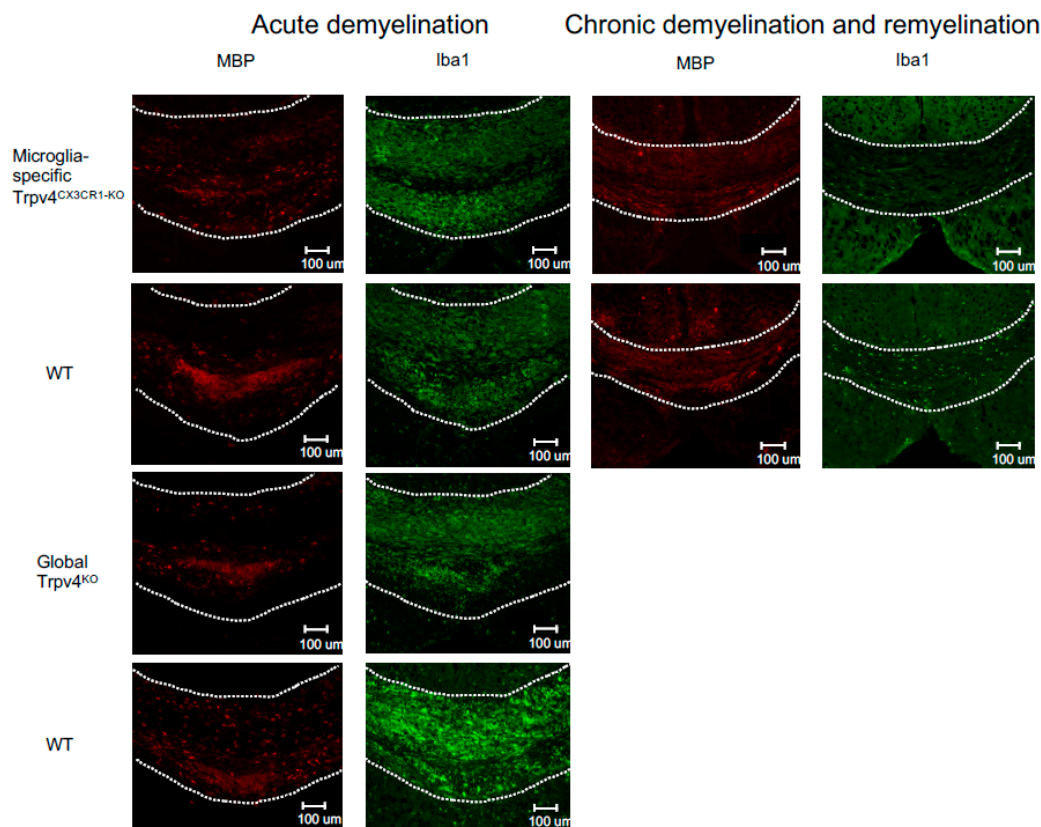


Figure 3. Representative immunofluorescent images of the splenium of the corpus callosum from microglia-specific Trpv4^{CX3CR1-KO} and global Trpv4^{KO} mice treated with cuprizone. Mice in each group were treated with either 6 weeks of cuprizone (acute demyelination protocol) or 12 weeks of cuprizone and 2 weeks of regular feed (chronic demyelination and remyelination protocol). All images were taken from the same reference point in the splenium of the corpus callosum. MBP staining (first and third column) visualizes myelin (in red). Iba1 staining (second and fourth column) visualizes microglia density (in green). The dotted white line demarcates the borders of the splenium of the corpus callosum. Scale bars indicate 100 μm. WT = wild type.

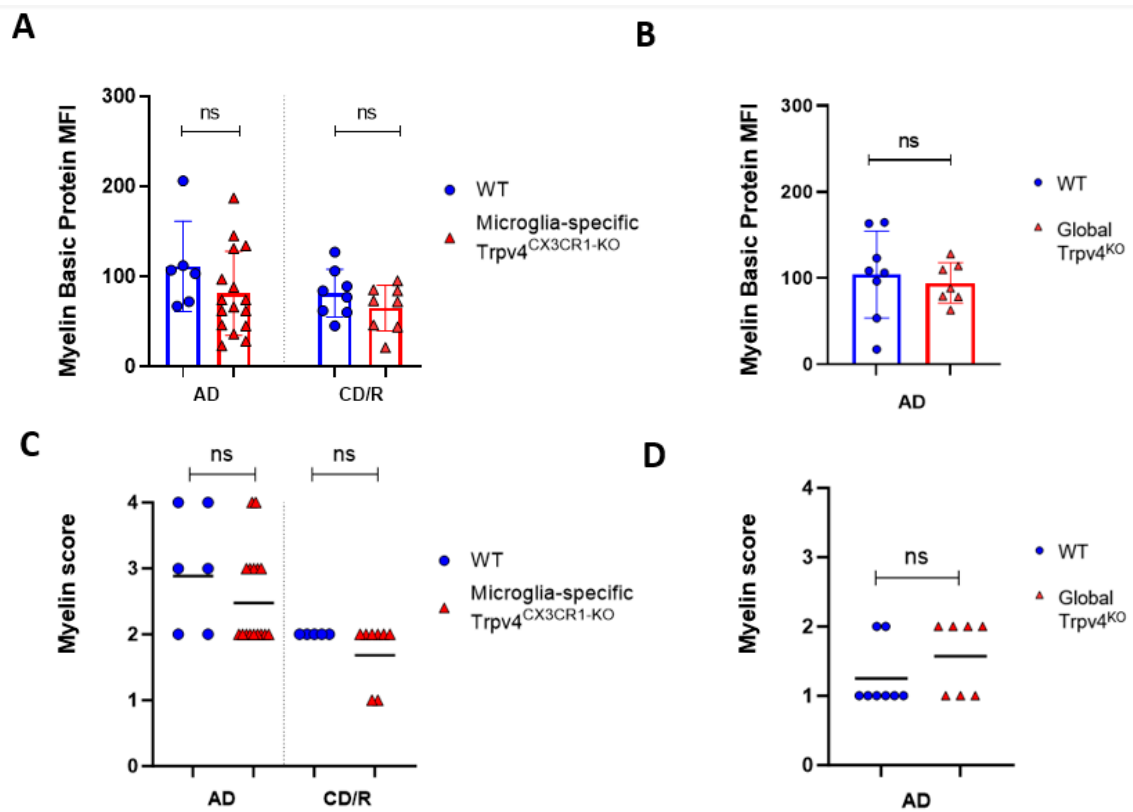


Figure 4. Global or microglial-specific loss of Trpv4 does not alter the degree of myelination following cuprizone administration. **(A)** Quantification of myelin content measured via myelin basic protein mean fluorescent intensity (MFI) after a 6-week acute demyelination and 14-week chronic demyelination/remyelination protocol in microglial-specific Trpv4^{KO} mice. **(B)** Quantification of myelin content via myelin basic protein MFI after a 6-week acute demyelination protocol in global Trpv4^{KO} mice. **(C)** Quantification of the myelin content via myelin scoring using the confocal images analyzed in **(A)**. **(D)** Quantification of the myelin content via myelin scoring using the confocal images analyzed in **(B)**. Myelin content was scored by a blinded rater as described previously (23) where a score of 0 indicates no demyelination detected, 1 indicates mild demyelination, 2 moderate demyelination, 3 indicates severe demyelination, and 4 indicates total demyelination. Statistical differences were determined using a Student's *t*-test. ns = non-significant. AD = acute demyelination protocol, CD/R = chronic demyelination/remyelination protocol, MFI = mean fluorescent intensity.

To more specifically investigate the impact of Trpv4 deletion on microglia in the cuprizone mouse model, we utilized mice with microglial-specific deletion of Trpv4, termed Trpv4^{CX3CR1-KO} mice, in both acute demyelination (6 weeks of cuprizone feed) and chronic demyelination/remyelination (Figure 2). We found no impact of microglia-specific loss of Trpv4 in the myelin content of the splenium of the corpus callosum after acute demyelination determined via MBP MFI (81.13 MFI in Trpv4^{CX3CR1-KO} mice (95% CI, 59.58–110.00) vs. 111.12 MFI in WT mice (95% CI, 59.19–164.00), $p = 0.20$). Further, there was no difference in MBP MFI at the chronic demyelination/remyelination stage between Trpv4^{CX3CR1-KO} and WT mice (65 MFI in Trpv4^{CX3CR1-KO} mice (95% CI, 43.73–86.16) vs. 81.25 MFI in WT mice (95% CI, 59.22–103.30), $p = 0.23$). These observations were also reflected by myelin scoring measures (acute demyelination: 2.56 in Trpv4^{CX3CR1-KO} mice (95% CI, 2.18–2.95) vs. 3.00 in WT mice (95% CI, 2.06–3.93), $p = 0.2507$, chronic demyelination/remyelination: 1.75 in KO mice (95% CI, 1.36–2.14) vs. 2.00 in WT mice (95% CI, 2.00–2.00), $p = 0.26$) (Figure 4). We then quantified the extent of microgliosis and found no difference in Iba1 staining within the splenium of the corpus callosum in either global Trpv4^{KO} or the microglia-specific Trpv4^{CX3CR1-KO} mice compared to WT controls (Figure 5).

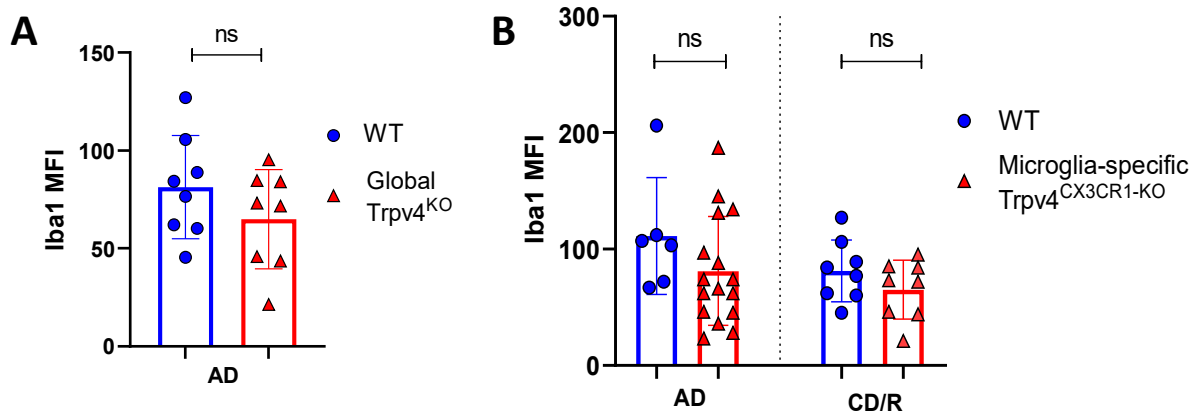


Figure 5. Global or microglial-specific loss of *Trpv4* does not alter the degree of microgliosis following cuprizone administration. (A) Quantification of the degree of microgliosis via mean fluorescent intensity after a 6-week demyelination protocol in global *Trpv4*^{KO}. (B) Quantification of the degree of microgliosis using Iba1 mean fluorescent intensity (MFI) measured via confocal microscopy after a 6-week acute demyelination and 14-week chronic demyelination/remyelination protocol in microglial-specific *Trpv4*^{CX3CR1-KO} mice. MFI was calculated using confocal images of fixed coronal sections of the splenium of the corpus callosum stained with Iba1. Statistical differences were determined using a Student's *t*-test. MFI = mean fluorescence intensity; ns = non-significant; AD = acute demyelination protocol; CD/R = chronic demyelination/remyelination protocol.

These results indicate that *Trpv4* deletion causes increased microglia phagocytosis *in vitro* but neither global nor microglia-specific *Trpv4* deletion alters the degree of myelin loss *in vivo* in the cuprizone mouse model. Additionally, *Trpv4* deletion does not alter the degree of microgliosis following cuprizone-mediated demyelination.

2.2. Global and Microglia-Specific *Trpv4* Deletion Does Not Impact EAE

Microglia are hypothesized to modulate neuroinflammation in MS and EAE via antigen presentation and pro-inflammatory cytokine secretion, potentially contributing to disease activity [7,23,24]. Given this immunomodulatory role of microglia, we explored the impact of TRPV4 on the EAE mouse model. We utilized global *Trpv4*^{KO} mice and microglia-specific *Trpv4* knockouts (*Trpv4*^{CX3CR1-KO} mice). We observed no change in EAE disease onset or severity in global *Trpv4*^{KO} mice and microglia-specific *Trpv4*^{KO} mice compared with WT mice. To account for any impact of *Trpv4* on severity of disease alone, we performed a separate set of analysis excluding mice that did not develop EAE. The results were similar, with no statistical differences between EAE severity in *Trpv4*^{KO} vs. WT mice (Figure 6A) or *Trpv4*^{CX3CR1-KO} vs. WT mice (Figure 6B). In our global *Trpv4*^{KO} cohort, there was an absolute increase in disease score between days 15–20 that subsequently dropped to the level of the disease score of WT mice. When this specific time interval was analyzed for statistical significance via Mann–Whitney U testing, it was found to be nonsignificant. These results demonstrate that neither global nor microglia-specific loss of *Trpv4* alters disease activity in EAE.

2.3. Expression of TRPV4 in MS Lesions, MS Normal-Appearing White Matter, and Control Tissue

We next analyzed MS brain tissue to determine if TRPV4 is differentially expressed in MS brain tissue. We examined expression of TRPV4 in chronic inactive lesions, active lesions, and NAWM in MS and compared it to NAWM from healthy controls (Table 1). To determine the amount of TRPV4 gene expression in MS lesions and MS normal appearing white matter, we isolated RNA from the brain tissue of MS patients and quantified the level of TRPV4 expression via quantitative PCR. We found no difference in TRPV4 expression between chronic inactive lesions, active lesions, MS NAWM and control tissue (Figure 7). We also found no difference overall in TRPV4 gene expression between MS and non-MS

(control) brain tissue, although there was a trend towards increased TRPV4 gene expression in MS brain tissue that did not achieve statistical significance. These results indicate that TRPV4 gene expression is similar between both MS lesions, MS NAWM, and healthy control tissue.

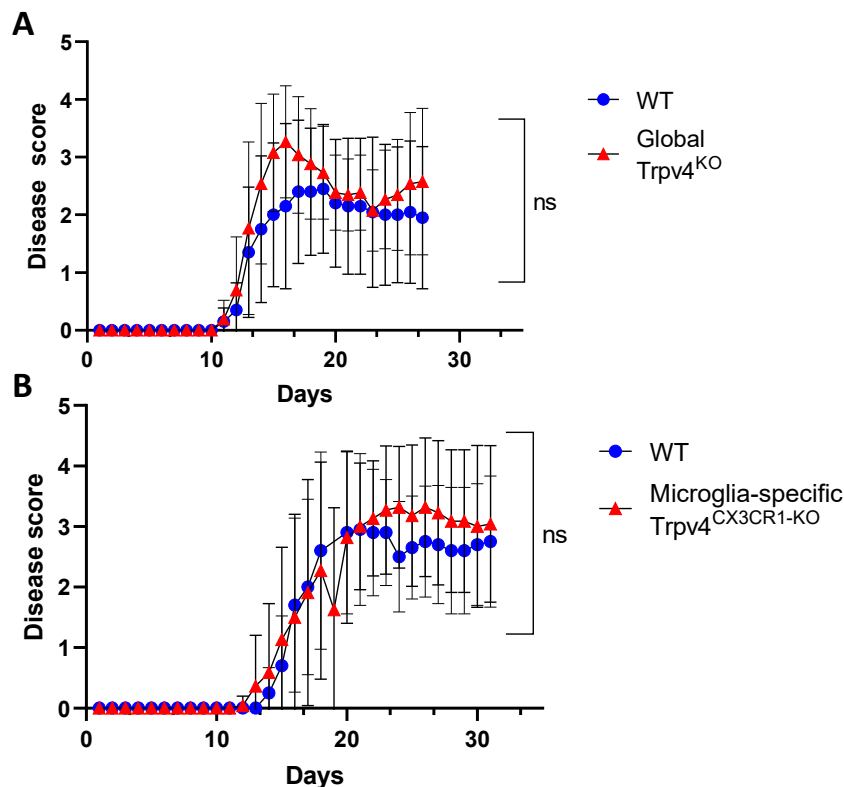


Figure 6. Microglia-specific $Trpv4^{CX3CR1-KO}$ and global $Trpv4^{KO}$ does not alter EAE disease severity. (A) EAE disease severity in wild type and CX3CR1 $Trpv4$ knockout mice. The wild type cohort contained 10 mice and the TRPV4 global knockout cohort contained 15 mice. Statistical differences were determined using the Mann–Whitney U test. (B) EAE disease severity in wild type and microglia-specific $Trpv4^{CX3CR1-KO}$ mice. The wild type cohort contained 10 mice and the CX3CR1 $Trpv4$ knockout cohort contained 13 mice. After the initial data analysis, the data was reanalyzed excluding mice that did not develop EAE and demonstrated similar results. The graphs above depict the results from the reanalysis. ns = non-significant, WT = wild type.

Table 1. Demographic information for MS cases and controls. Demographic information on the multiple sclerosis cases and healthy control cases from which brain tissue was sampled for measurement of TRPV4 gene expression via real-time PCR.

Sex/Age	MS Subtype	PMI (Hours)	Cause of Death	Lesion Type
M/60	SPMS	9	Respiratory failure	Active
F/45	PPMS	4	Pneumonia	Chronic active
F/50	SPMS	20	Unknown	Active, chronic inactive
M/35	PPMS	10	Unknown	Chronic inactive
F/54	SPMS	8	Pneumonia	Chronic inactive
F/69	PPMS	5	Metastatic colon cancer	Active
F/79	RRMS	8	Pulmonary edema	NAWM, chronic inactive
F/95	SPMS	9	Pulmonary edema	NAWM
F/41	RRMS	12	Complications from T1D	NAWM
F/54	SPMS	7	Pneumonia	Chronic inactive

Table 1. Cont.

Sex/Age	MS Subtype	PMI (Hours)	Cause of Death	Lesion Type
F/86	PPMS	12	Cardiac arrest	NAWM
F/66	Unknown	29	Unknown	NAWM
F/39	HC	4	CNS lymphoma	NA
F/56	HC	18	Myocardial infarction	NA
F/69	HC	43	Sepsis	NA
M/41	HC	24	Heart failure	NA

PMI = post-mortem interval; T1D = Type 1 diabetes; NAWM = Normal appearing white matter; NA = not applicable. PPMS = primary progressive multiple sclerosis, SPMS = secondary progressive multiple sclerosis, RRMS = relapsing–remitting multiple sclerosis.

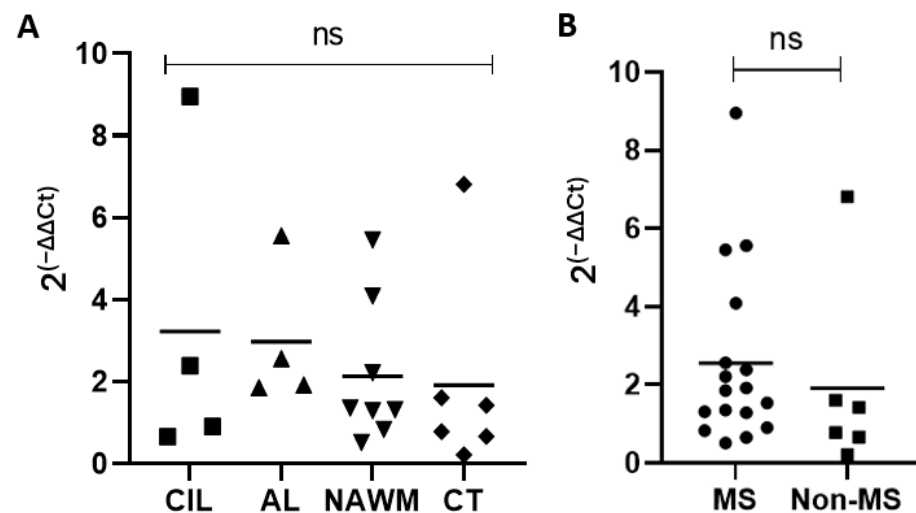


Figure 7. TRPV4 gene expression does not differ between MS lesions, MS normal appearing white matter, and healthy control tissue. (A) TRPV4 gene expression in chronic inactive MS lesions, active MS lesions, MS NAWM, and healthy control brain tissue. (B) Combined analysis of TRPV4 gene expression in MS lesions + MS NAWM (MS) and healthy control brain tissue (Non-MS). Y axis for both graphs indicates relative fold expression change in TRPV4 compared to GAPDH. Statistical differences determined using a Student's *t*-test. ns = non-significant. CIL = chronic inactive lesions, AL = active lesions, NAWM = MS normal appearing white matter, CT = control tissue.

3. Discussion

Our results indicate that loss of TRPV4 increases microglia phagocytosis *in vitro* but does not alter the degree of demyelination, remyelination or microgliosis in the cuprizone model of MS. Similarly, *in vivo* loss of TRPV4, globally or selectively in microglia, did not affect disease severity in the active EAE model of MS. Consistent with these *in vivo* observations, no difference in *TRPV4* gene expression was observed between MS brain tissue and control tissue, indicating that *TRPV4* is not differentially expressed in the MS brain. Overall, these findings indicate that TRPV4 modulates microglia activity, but this effect is unlikely to have an impact on the pathogenesis of MS.

Our study employed microglia-specific *Trpv4* genetic knockouts to study the effect of TRPV4 in microglia *in vitro* and on the MS mouse models of cuprizone and EAE. Our *in vitro* findings of increased phagocytosis following TRPV4^{KO} are consistent with prior research demonstrating that TRPV4 activation decreased LPS-induced microglia activation [25]. Our results are consistent with the lack of an effect of global TRPV4^{KO} on EAE observed previously [16].

There are many possible explanations for the seemingly opposing findings of increased microglia phagocytosis *in vitro* without an apparent effect of TRPV4 deletion in MS mouse models. Microglia are hypothesized to play a multifaceted role in MS, performing both pro-inflammatory [8] and anti-inflammatory [26] roles throughout the MS disease

course. Additionally, microglia have been found to both enhance [26,27] and impair [28] remyelination in MS depending on their cytokine expression profile and phenotype. Given the potential dual role of microglia in MS, loss of TRPV4 may lead to equal and opposite effects on microglia causing a net neutral result. For example, if TRPV4 increased microglia phagocytosis in MS, as we observed in vitro, but also increased expression of pro-inflammatory cytokines, this would lead to increased myelin clearance, subsequently decreasing inflammation and promoting remyelination. However, this would simultaneously lead to increased neuroinflammation through the secretion of pro-inflammatory cytokines, leading to decreased remyelination. The net result would be a comparable level of disease pathology.

Another possible explanation is that TRPV4 modulation alters the phenotype of homeostatic microglia but does not impact microglia in the context of cuprizone-mediated demyelination, EAE, and MS. This has been observed experimentally with endothelial cells in which inhibition of TRPV4 under homeostatic conditions leads to increased endothelial cell permeability and increased blood–brain barrier permeability but in states of inflammation, such as EAE, this effect does not occur [16]. A final explanation is that the effect of increased microglia TRPV4-mediated phagocytosis is negligible in the larger context of MS, where other disease processes predominate.

Our findings conflict with a previous study by Liu et al. 2018 that found that intracerebroventricular infusion of a TRPV4 antagonist in mice receiving cuprizone diminished the degree of demyelination and reduced the number of astrocytes and microglia in the corpus callosum [22]. This difference in outcome may be related to the difference in mechanism of TRPV4 deletion employed in our respective studies. Liu et al. performed transient TRPV4 antagonism using intracerebroventricular infusion of a TRPV4 antagonist. In contrast, in our experiments a constitutive global and microglia-specific TRPV4 knockout genetic approach were used to assess in vivo function. This difference could result in temporal, spatial, and cell-specific differences between our two models which could then translate to clinical differences. Possible disparities attributable to the mechanism of TRPV4 loss of function is supported by prior research which demonstrated that pharmacologic TRPV4 inhibition with an TRPV4 antagonist resulted in changes to microglia morphology and motility but constitutive, global deletion of *Trpv4* had no effect on microglia [29]. Additionally, CNS delivery of a TRPV4 antagonist produces a localized effect in the CNS. In contrast, our global knockouts have systemic effects which may lead to alterations in cells within the periphery that may negate the neuroprotective effects occurring locally within the CNS. For example, a previously described shift in peripheral macrophages towards a pro-inflammatory phenotype in TRPV4^{KO} mice [30] could lead to a higher infiltration of macrophages in the CNS and a higher degree of neuroinflammation. This infiltration of pro-inflammatory myeloid cells into the CNS could obviate local neuroprotective effects from TRPV4 loss in microglia. Finally, our microglia-specific *Trpv4*^{CX3CR1-KO} selectively deletes *Trpv4* in CNS microglia, which results in primary changes only to microglia, whereas local pharmacologic TRPV4 antagonism causes changes in all CNS cells expressing TRPV4. Therefore, if local antagonism achieves a therapeutic benefit by blocking TRPV4 on CNS cells other than microglia, then this benefit would not be observed in microglia-specific *Trpv4*^{CX3CR1-KO} mice.

Our research has several limitations, including narrow in vitro experimental approaches. We chose to focus our experiments primarily on the effect of TRPV4 loss in mouse models of MS and therefore did not conduct further in vitro assays using microglia from TRPV4^{KO} mice. However, further in vitro assays may help elucidate the mechanism by which loss of TRPV4 induces changes in microglia and demonstrate the broader effects of these changes. Additionally, a lack of techniques with greater resolution for quantifying myelination (e.g., 3D electron microscopy) could be one limitation in interpreting the extent to which TRPV4 function in microglial affects demyelination and remyelination in vivo. Nevertheless, we chose to quantify myelination in our cuprizone mice via immunohistochemical staining with MBP and solochrome cyanine which demonstrated

consistency in staining patterns across the two stains, increasing our confidence in the results (Supplementary Figure S1).

Overall, the lack of any significant change in myelin content, microgliosis, or disease severity in the cuprizone and EAE mouse models with global and microglia-specific loss of TRPV4 indicates that TRPV4 is unlikely to play a prominent role in MS pathogenesis. This is supported by a lack of differential gene expression of TRPV4 in the brain tissue of MS patients. It is possible that the direct application of a TRPV4 antagonist to the CNS results in a differential effect compared to the constitutive deletion of *Trpv4*, leaving open the possibility of a therapeutic potential for transient TRPV4 antagonism. This warrants further evaluation through experiments that compare the functional and morphological differences between transient and constitutive loss of TRPV4 in microglia as well as other CNS cells such as endothelial cells. We cannot rule out the possibility that a toxic gain of function of TRPV4 could contribute to disease pathogenesis in MS. Our study specifically examined *Trpv4* deletion through animal modeling and in vitro experiments and therefore cannot comment specifically on the impact of toxic gain of function of TRPV4. However, our human data did not demonstrate an increased expression of TRPV4 within MS tissue, making toxic gain of function of TRPV4 less likely. Cell-based or in vivo experiments that evaluate the phagocytosis of myelin in microglia deficient in, or over-expressing TRPV4 could provide further information about how TRPV4 modulates myelin-specific phagocytosis. These experiments may offer insight into the mechanisms by which TRPV4 mediates functional changes in neuroinflammation.

4. Materials and Methods

4.1. Microglia Cultures

Primary microglia were obtained from mixed cultures prepared from the hippocampi and cerebral cortices of TRPV4^{KO} mice and wild type C57BL/6J mice at postnatal day (P)1-3 as previously described [31]. Microglial cells were isolated by shaking flasks for 45 min at 230 RPM on day 10 after plating. Cells were then seeded on poly L-ornithine (Sigma; St. Louis, MO, USA) pre-coated wells at a density of 1.53105 cell/mL in DMEM containing 20% heat-inactivated fetal bovine serum. For biological replication, ten different mice and two sets of cultures were used in each experimental group.

4.2. Microglia Phagocytosis Assay

Red fluorescent latex beads (Sigma, L2778; St. Louis, MO, USA) were pre-opsionized with FBS for one hour and then co-cultured with microglia derived from *Trpv4* –/– mice (global *Trpv4*^{KO}) and wild type microglia in DMEM using 100,000 microglia per sample. Microglia were incubated for three hours with the latex beads and then fixed and stained for Iba1 (Wako; Richmond, VA, USA). Microglia were analyzed using a Zeiss LSM880 Confocal Laser Scanning Microscope (Carl Zeiss Microscopy; White Plains, NY, USA) and the number of internally phagocytosed fluorescent beads per microglia were counted. For technical replication, 10 separate microscopic fields with at least 500 microglia total were quantified per cell culture.

4.3. Mice

All animal experiments followed the guidelines of the National Institutes of Health (NIH, New York, NY, USA), and all animal protocols were approved by the Institutional Animal Care and Use Committees (IACUC) of Washington University in St. Louis. Mice were housed in a temperature- and humidity-controlled animal facility employing a 12 h light/dark cycle with food and water available ad libitum. Global *Trpv4*^{KO} mice [32] and *Trpv4*^{f/f}; *CX3CR1*^{CreERT2} mice (microglia-specific *Trpv4*^{CX3CR1-KO} mice) were bred in-house (HH lab) [21,33]. Microglia-specific *Trpv4*^{CX3CR1-KO} mice were treated with 100 mg/kg of tamoxifen administered via oral gavage for 5 consecutive days to induce Cre-Lox recombination. Genotypes were determined by PCR from the DNA extracted from tail tips. *Trpv4* flox alleles were genotyped by the primer set (5'-CCAAGACAGGCAAGATCGGG-3'; 5'-

CTGACTGATGGAGGTTGGGT-3'). Genotyping CX3CR1^{CreERT2} mice utilized the following primers: 5'-CCAAGACAGGCAAGATCGGG-3'; 5'-CTGACTGATGGAGGTTGGGT-3'. The recombined *Trpv4* allele in microglia-specific *Trpv4*^{CX3CR1-KO} mice following tamoxifen administration was genotyped using primers (5'-ACCCTCATTTTGGTCCATCC-3'; 5'-CTGACTGATGGAGGTTGGGT-3'). Microglia were isolated from microglia-specific *Trpv4*^{CX3CR1-KO} mice via FACS sorting and genotyped to confirm successful recombination (Supplementary Figure S2). Both females and males were used in this study. WT litter mates served as controls for all animal experiments.

4.4. EAE Induction and Clinical Score Assessment

Active EAE was induced as previously described [34]. Briefly, mice were subcutaneously injected with 200 µg of MOG_{35–55} peptide (Genscript, RP10245) emulsified in incomplete Freud's adjuvant (Sigma, F5506; St. Louis, MO, USA) with mycobacterium tuberculosis H37Ra (BD Difco, BD 231141; Pittsburgh, PA, USA) and intraperitoneally injected with 200 ng of Pertussis Toxin (List Biological Laboratories, Campbell, CA, USA). All EAE mice were monitored daily and scored using a clinical scale from 0 to 5 (0: no abnormality; 1: limp tail; 2: limp tail and hind leg weakness; 3: limp tail and complete paralysis of hind legs; 4: hind leg and partial front leg paralysis; 5: moribund). For biological replication, the TRPV4 global knockout cohort contained 15 mice, the CX3CR1 *Trpv4* knockout cohort contained 13 mice, and the wild type cohorts each contained 10 mice.

4.5. Cuprizone-Induced Acute Demyelination and Chronic Demyelination/Remyelination Models

Cuprizone is a copper-chelating mitochondrial toxin that causes oligodendroglial cell death and demyelination by an inhibition of complex IV of the mitochondrial respiratory chain and induces megamitochondria in the mouse brain. To induce acute demyelination in the CNS, global TRPV4^{KO} and microglia-specific *Trpv4*^{CX3CR1-KO} mice, standard 0.3% cuprizone diet in chow (Sigma; St. Louis, MO, USA) was provided for a period of six weeks as previously described [35]. Another group of microglia-specific *Trpv4*^{CX3CR1-KO} mice were fed a standard 0.3% cuprizone diet in chow (Sigma; St. Louis, MO, USA) for 12 weeks followed by two weeks of regular feed (Gateway lab supply, St Louis, MO, USA) to model chronic demyelination and subsequent remyelination as previously described [36]. The body weight of all mice was monitored once a week. For biological replication, the global TRPV4^{KO} cohort that underwent acute demyelination contained 8 mice and the wild type cohort contained 8 mice. For the microglia-specific *Trpv4*^{CX3CR1-KO} mice, the knockout cohort that underwent acute demyelination contained 8 mice and the wild type cohort contained 8 mice, and the knockout cohort that underwent chronic demyelination and remyelination contained 15 mice and the wild type cohort contained 8 mice.

4.6. Immunohistochemistry

The mice were anesthetized and perfused transcardially with PBS and 4% PFA. The spinal cord and brain were dissected and post fixed in 4% paraformaldehyde (PFA) overnight at 4 °C, followed by equilibration in 30% sucrose. Subsequently, 20 µm cryosections were collected from brains at the splenium of the corpus callosum and stored at −20 °C. Sections were incubated with primary antibodies overnight at 4 °C (MBP: Abcam; Eugene, Oregon Iba1: Wako; Richmond, VA, USA) and washed and incubated with fluorescently conjugated secondary donkey anti-rabbit IgG 488 (ThermoFisher; Waltham, MA, USA) or donkey anti-rat IgG 647 (Invitrogen; Rockford, IL, USA) antibodies for 1 h at room temperature. Images were collected and analyzed using a Zeiss LSM880 Confocal Laser Scanning Microscope.

4.7. Myelin Content Quantification

Myelin content was quantified by both mean fluorescent intensity and blinded myelin scoring. Serial sections of the corpus callosum at approximately −2.2 to −2.4 mm posterior from Bregma were collected for each mouse, stained with MBP (Abcam; Eugene, OR, USA),

and analyzed using a Zeiss LSM880 Confocal Laser Scanning Microscope. For technical replication, two serial 30 μm corpus callosum slices at approximately -2.2 to -2.4 mm posterior from Bregma were collected and stained for each mouse. Mean fluorescent intensity was calculated after outlining the corpus callosum in each image and averaging the signal intensity of both slices. Myelin content in each image was also scored by a blinded rater from an independent lab as described previously [37], where a score of 0 indicates no demyelination detected, 1 indicates mild demyelination, 2 moderate demyelination, 3 indicates severe demyelination, and 4 indicates total demyelination.

4.8. Solochrome Cyanine Staining

For myelin staining, sections were air-dried and carried through the following sequence: 95% ethanol, 95% ethanol/formaldehyde; 95% ethanol, 70% ethanol, dH_2O , then to the solochrome staining solution (80 mL of Solochrome stock solution (1.5% solochrome, 2.5% *v/v* sulfuric acid), 320 mL dH_2O , 100 mL 4% ferric ammonium sulfate) at room temperature. Sections were then rinsed with tap water, differentiated in potassium ferricyanide-sodium borate, and rinsed in tap water again. Differentiated sections were counterstained lightly with neutral red, dehydrated, cleared in xylene and cover slipped. For technical replication, three serial 30 μm corpus callosum slices at approximately -2.2 to -2.4 mm posterior from Bregma were collected and stained.

4.9. Quantification of TRPV4 Gene Expression in MS Brain Tissue

Fresh frozen tissue blocks were obtained from the John L. Trotter MS tissue biorepository at Washington University from the brain tissue of MS patients (demographics listed in Table 1). MS lesions and healthy control tissue were obtained from periventricular cerebral white matter. RNA from tissue sections was extracted with the RNeasy kit (QIAGEN; Germantown, MD, USA) according to the manufacturer's instructions. cDNA was created using SuperScript IV Reverse Transcriptase according to the manufacturer's instructions. Quantitative real-time PCR was carried out using TaqMan Fast Advanced Master Mix (ThermoFisher; Waltham, MA, USA) on an ABI 7900HT instrument. *GAPDH* was used as the normalization control and the DDCT method was used to quantify gene expression.

4.10. Statistical Analysis

All statistical analyses were performed using GraphPad Prism software, V 9.0 (GraphPad Software, La Jolla, CA, USA). Normality was tested by the Shapiro–Wilk test and data are shown as the mean and standard deviation. Statistical difference in microglia phagocytosis was determined using a nested Student's *t*-test. Difference in EAE disease course was determined using the Mann–Whitney U test. Difference in *TRPV4* gene expression in MS and control brain tissue was determined using one-way ANOVA. In all other experiments, comparison of mean values was conducted using the Student's *t*-test. For all statistical tests, two-sided *p*-values of 0.05 or less were considered significant.

Supplementary Materials: The following supporting information can be downloaded at: <https://www.mdpi.com/article/10.3390/ijms242317097/s1>.

Author Contributions: Conceptualization, G.F.W., J.P.H. and H.H.; methodology, J.P.H., B.B., A.S.A., L.D., L.P., Y.Z. and J.F.; software, J.P.H. and A.J.S.; validation, J.P.H. and A.J.S.; formal analysis, J.P.H., A.J.S. and S.H.D.; resources, G.F.W.; data curation, J.P.H.; writing—original draft preparation, J.P.H. and G.F.W.; writing—review and editing, J.P.H. and G.F.W.; visualization, J.P.H.; supervision, F.F. and G.F.W.; project administration, G.F.W.; funding acquisition, G.F.W. and H.H. All authors have read and agreed to the published version of the manuscript.

Funding: G.F.W. and H.H. were supported by R01NS106289 from the National Institute of Neurological Disorders and Stroke (NINDS), J.P.H. was supported by R25NS090978, and A.J.S. was supported by the National Multiple Sclerosis Society (RG-1807-32053).

Institutional Review Board Statement: The study was conducted in accordance with all guidelines of Washington University's Institutional Review Board and Institutional Animal Care and Use Committee (Animal Welfare Assurance number is A-3381-01 and approval date is 19 August 2020).

Informed Consent Statement: Not applicable.

Data Availability Statement: The data presented in this study are openly available on request from the corresponding author at synapse.org (syn52309481).

Acknowledgments: We would like to thank Anne H. Cross for conceptual guidance and experimental support via the John L. Trotter MS repository.

Conflicts of Interest: The authors declare no conflict of interest. The funders had no role in the design of the study; in the collection, analyses, or interpretation of data; in the writing of the manuscript; or in the decision to publish the results.

References

1. Walton, C.; King, R.; Rechtman, L.; Kaye, W.; Leray, E.; Marrie, R.A.; Robertson, N.; La Rocca, N.; Uitdehaag, B.; Van Der Mei, I.; et al. Rising prevalence of multiple sclerosis worldwide: Insights from the Atlas of MS. *Mult. Scler. J.* **2020**, *26*, 1816–1821. [[CrossRef](#)] [[PubMed](#)]
2. Ghasemi, N.; Razavi, S.; Nikzad, E. Multiple sclerosis: Pathogenesis, symptoms, diagnoses and cell-based therapy. *Cell J.* **2017**, *19*, 1. [[PubMed](#)]
3. Frischer, J.M.; Bramow, S.; Dal-Bianco, A.; Lucchinetti, C.F.; Rauschka, H.; Schmidbauer, M.; Laursen, H.; Sorensen, P.S.; Lassmann, H. The relation between inflammation and neurodegeneration in multiple sclerosis brains. *Brain* **2009**, *132*, 1175–1189. [[CrossRef](#)]
4. Baker, D.; O'Neill, J.; Turk, J. Cytokines in the central nervous system of mice during chronic relapsing experimental allergic encephalomyelitis. *Cell. Immunol.* **1991**, *134*, 505–510. [[CrossRef](#)] [[PubMed](#)]
5. Bettelli, E.; Sullivan, B.; Szabo, S.J.; Sobel, R.A.; Glimcher, L.H.; Kuchroo, V.K. Loss of T-bet, but not STAT1, prevents the development of experimental autoimmune encephalomyelitis. *J. Exp. Med.* **2004**, *200*, 79–87. [[CrossRef](#)]
6. Dal-Bianco, A.; Grabner, G.; Kronnerwetter, C.; Weber, M.; Höftberger, R.; Berger, T.; Auff, E.; Leutmezer, F.; Trattinig, S.; Lassmann, H.; et al. Slow expansion of multiple sclerosis iron rim lesions: Pathology and 7 T magnetic resonance imaging. *Acta Neuropathol.* **2017**, *133*, 25–42. [[CrossRef](#)] [[PubMed](#)]
7. Boyle, E.; McGeer, P. Cellular immune response in multiple sclerosis plaques. *Am. J. Pathol.* **1990**, *137*, 575.
8. Zrzavy, T.; Hametner, S.; Wimmer, I.; Butovsky, O.; Weiner, H.L.; Lassmann, H. Loss of 'homeostatic' microglia and patterns of their activation in active multiple sclerosis. *Brain* **2017**, *140*, 1900–1913. [[CrossRef](#)]
9. Singh, S.; Metz, I.; Amor, S.; van der Valk, P.; Stadelmann, C.; Brück, W. Microglial nodules in early multiple sclerosis white matter are associated with degenerating axons. *Acta Neuropathol.* **2013**, *125*, 595–608. [[CrossRef](#)]
10. Ramaglia, V.; Hughes, T.R.; Donev, R.M.; Ruseva, M.M.; Wu, X.; Huitinga, I.; Baas, F.; Neal, J.W.; Morgan, B.P. C3-dependent mechanism of microglial priming relevant to multiple sclerosis. *Proc. Natl. Acad. Sci. USA* **2012**, *109*, 965–970. [[CrossRef](#)]
11. Neumann, H.; Kotter, M.; Franklin, R. Debris clearance by microglia: An essential link between degeneration and regeneration. *Brain* **2009**, *132*, 288–295. [[CrossRef](#)]
12. Lampron, A.; Laroche, A.; Laflamme, N.; Préfontaine, P.; Plante, M.-M.; Sánchez, M.G.; Yong, V.W.; Stys, P.K.; Tremblay, M.; Rivest, S. Inefficient clearance of myelin debris by microglia impairs remyelinating processes. *J. Exp. Med.* **2015**, *212*, 481–495. [[CrossRef](#)]
13. Kanju, P.; Liedtke, W. Pleiotropic function of TRPV4 ion channels in the central nervous system. *Exp. Physiol.* **2016**, *101*, 1472–1476. [[CrossRef](#)] [[PubMed](#)]
14. White, J.P.; Cibelli, M.; Urban, L.; Nilius, B.; McGeown, J.G.; Nagy, I. TRPV4: Molecular conductor of a diverse orchestra. *Physiol. Rev.* **2016**, *96*, 911–973. [[CrossRef](#)] [[PubMed](#)]
15. Rajasekhar, P.; Poole, D.P.; Veldhuis, N.A. Role of nonneuronal TRPV4 signaling in inflammatory processes. *Adv. Pharmacol.* **2017**, *79*, 117–139. [[PubMed](#)]
16. Rosenkranz, S.C.; Shaposhnykov, A.; Schnapauff, O.; Epping, L.; Vieira, V.; Heidermann, K.; Schattling, B.; Tsvilovskyy, V.; Liedtke, W.; Meuth, S.G.; et al. TRPV4-mediated regulation of the blood brain barrier is abolished during inflammation. *Front. Cell Dev. Biol.* **2020**, *8*, 849. [[CrossRef](#)]
17. Liedtke, W. TRPV4 plays an evolutionary conserved role in the transduction of osmotic and mechanical stimuli in live animals. *J. Physiol.* **2005**, *567*, 53–58. [[CrossRef](#)] [[PubMed](#)]
18. Stampanoni Bassi, M.; Gentile, A.; Iezzi, E.; Zagaglia, S.; Musella, A.; Simonelli, I.; Gilio, L.; Furlan, R.; Finardi, A.; Marfia, G.A.; et al. Transient receptor potential vanilloid 1 modulates central inflammation in multiple sclerosis. *Front. Neurol.* **2019**, *10*, 30. [[CrossRef](#)]
19. Redmon, S.N.; Yarishkin, O.; Lakk, M.; Jo, A.; Mustafić, E.; Tvrdik, P.; Križaj, D. TRPV4 channels mediate the mechanoreponse in retinal microglia. *Glia* **2021**, *69*, 1563–1582. [[CrossRef](#)]

20. Wang, Z.; Zhou, L.; An, D.; Xu, W.; Wu, C.; Sha, S.; Li, Y.; Zhu, Y.; Chen, A.; Du, Y.; et al. TRPV4-induced inflammatory response is involved in neuronal death in pilocarpine model of temporal lobe epilepsy in mice. *Cell Death Dis.* **2019**, *10*, 386. [[CrossRef](#)]
21. Luo, J.; Feng, J.; Yu, G.; Yang, P.; Mack, M.R.; Du, J.; Yu, W.; Qian, A.; Zhang, Y.; Liu, S.; et al. Transient receptor potential vanilloid 4-expressing macrophages and keratinocytes contribute differentially to allergic and nonallergic chronic itch. *J. Allergy Clin. Immunol.* **2018**, *141*, 608–619.e7. [[CrossRef](#)]
22. Liu, M.; Liu, X.; Wang, L.; Wang, Y.; Dong, F.; Wu, J.; Qu, X.; Liu, Y.; Liu, Z.; Fan, H.; et al. TRPV4 inhibition improved myelination and reduced glia reactivity and inflammation in a cuprizone-induced mouse model of demyelination. *Front. Cell. Neurosci.* **2018**, *12*, 392. [[CrossRef](#)]
23. Almolda, B.; González, B.; Castellano, B. Activated microglial cells acquire an immature dendritic cell phenotype and may terminate the immune response in an acute model of EAE. *J. Neuroimmunol.* **2010**, *223*, 39–54. [[CrossRef](#)] [[PubMed](#)]
24. Murphy, C.; Lalor, S.J.; Lynch, M.A.; Mills, K.H. Infiltration of Th1 and Th17 cells and activation of microglia in the CNS during the course of experimental autoimmune encephalomyelitis. *Brain Behav. Immun.* **2010**, *24*, 641–651. [[CrossRef](#)]
25. Konno, M.; Shirakawa, H.; Iida, S.; Sakimoto, S.; Matsutani, I.; Miyake, T.; Kageyama, K.; Nakagawa, T.; Shibasaki, K.; Kaneko, S. Stimulation of transient receptor potential vanilloid 4 channel suppresses abnormal activation of microglia induced by lipopolysaccharide. *Glia* **2012**, *60*, 761–770. [[CrossRef](#)]
26. Peferoen, L.A.; Vogel, D.Y.; Ummenthum, K.; Breur, M.; Heijnen, P.D.; Gerritsen, W.H.; Peferoen-Baert, R.M.; van der Valk, P.; Dijkstra, C.D.; Amor, S. Activation status of human microglia is dependent on lesion formation stage and remyelination in multiple sclerosis. *J. Neuropathol. Exp. Neurol.* **2015**, *74*, 48–63. [[CrossRef](#)]
27. Harnisch, K.; Teuber-Hanselmann, S.; Macha, N.; Mairinger, F.; Fritsche, L.; Soub, D.; Meinl, E.; Junker, A. Myelination in multiple sclerosis lesions is associated with regulation of bone morphogenetic protein 4 and its antagonist noggin. *Int. J. Mol. Sci.* **2019**, *20*, 154. [[CrossRef](#)] [[PubMed](#)]
28. Prinz, M.; Priller, J. Microglia and brain macrophages in the molecular age: From origin to neuropsychiatric disease. *Nat. Rev. Neurosci.* **2014**, *15*, 300–312. [[CrossRef](#)] [[PubMed](#)]
29. Beeken, J.; Mertens, M.; Stas, N.; Kessels, S.; Aerts, L.; Janssen, B.; Mussen, F.; Pinto, S.; Vennekens, R.; Rigo, J.; et al. Acute inhibition of transient receptor potential vanilloid-type 4 cation channel halts cytoskeletal dynamism in microglia. *Glia* **2022**, *70*, 2157–2168. [[CrossRef](#)]
30. Scheraga, R.G.; Abraham, S.; Niese, K.A.; Southern, B.D.; Grove, L.M.; Hite, R.D.; McDonald, C.; Hamilton, T.A.; Olman, M.A. TRPV4 mechanosensitive ion channel regulates lipopolysaccharide-stimulated macrophage phagocytosis. *J. Immunol.* **2016**, *196*, 428–436. [[CrossRef](#)]
31. Lian, H.; Roy, E.; Zheng, H. Protocol for primary microglial culture preparation. *Bio-Protocol* **2016**, *6*, e1989. [[CrossRef](#)] [[PubMed](#)]
32. Suzuki, M.; Mizuno, A.; Kodaira, K.; Imai, M. Impaired pressure sensation in mice lacking TRPV4. *J. Biol. Chem.* **2003**, *278*, 22664–22668. [[CrossRef](#)] [[PubMed](#)]
33. Hu, X.; Du, L.; Liu, S.; Lan, Z.; Zang, K.; Feng, J.; Zhao, Y.; Yang, X.; Xie, Z.; Wang, P.L.; et al. A TRPV4-dependent neuroimmune axis in the spinal cord promotes neuropathic pain. *J. Clin. Investig.* **2023**, *133*, e161507. [[CrossRef](#)] [[PubMed](#)]
34. Wu, G.F.; Shindler, K.S.; Allenspach, E.J.; Stephen, T.L.; Thomas, H.L.; Mikesell, R.J.; Cross, A.H.; Laufer, T.M. Limited sufficiency of antigen presentation by dendritic cells in models of central nervous system autoimmunity. *J. Autoimmun.* **2011**, *36*, 56–64. [[CrossRef](#)]
35. Sachs, H.H.; Bercury, K.K.; Popescu, D.C.; Narayanan, S.P.; Macklin, W.B. A new model of cuprizone-mediated demyelination/remyelination. *ASN Neuro* **2014**, *6*, 1759091414551955. [[CrossRef](#)]
36. Lindner, M.; Fokuhl, J.; Linsmeier, F.; Trebst, C.; Stangel, M. Chronic toxic demyelination in the central nervous system leads to axonal damage despite remyelination. *Neurosci. Lett.* **2009**, *453*, 120–125. [[CrossRef](#)]
37. Steelman, A.J.; Thompson, J.P.; Li, J. Demyelination and remyelination in anatomically distinct regions of the corpus callosum following cuprizone intoxication. *Neurosci. Res.* **2012**, *72*, 32–42. [[CrossRef](#)]

Disclaimer/Publisher’s Note: The statements, opinions and data contained in all publications are solely those of the individual author(s) and contributor(s) and not of MDPI and/or the editor(s). MDPI and/or the editor(s) disclaim responsibility for any injury to people or property resulting from any ideas, methods, instructions or products referred to in the content.